1994-09

A mathematical analysis of the Janus combat simulation weather effects models and sensitivity analysis of sky-to-ground brightness ratio on target detection

Shorts, Vincient F.

Monterey, California. Naval Postgraduate School

NAVAL POSTGRADUATE SCHOOL
Monterey, California

THESIS

A MATHEMATICAL ANALYSIS OF THE JANUS COMBAT SIMULATION WEATHER EFFECTS MODELS AND SENSITIVITY ANALYSIS OF SKY-TO-GROUND BRIGHTNESS RATIO ON TARGET DETECTION

by

Vincient F. Shorts

September 1994

Thesis Co-Advisors: Bard Mansager
Maurice Weir

Approved for public release; distribution is unlimited

REPORT DOCUMENTATION PAGE

Form Approved OMB No. 0704-0188

1. AGENCY USE ONLY *(Leave blank)*	2. REPORT DATE	3. REPORT TYPE AND DATES COVERED
	September 1994	Master's Thesis

4. TITLE AND SUBTITLE: A MATHEMATICAL ANALYSIS OF THE JANUS COMBAT SIMULATION WEATHER EFFECTS MODELS AND SENSITIVITY ANALYSIS OF SKY-TO-GROUND BRIGHTNESS RATIO ON TARGET DETECTION	5. FUNDING NUMBERS
6. AUTHOR(S) Vincient F. Shorts	
7. PERFORMING ORGANIZATION NAME(S) AND ADDRESS(ES) Naval Postgraduate School Monterey CA 93943-5000	8. PERFORMING ORGANIZATION REPORT NUMBER
9. SPONSORING/MONITORING AGENCY NAME(S) AND ADDRESS(ES)	10. SPONSORING/MONITORING AGENCY REPORT NUMBER

11. SUPPLEMENTARY NOTES The views expressed in this thesis are those of the author and do not reflect the official policy or position of the Department of Defense or the U.S. Government.

12a. DISTRIBUTION/AVAILABILITY STATEMENT	12b. DISTRIBUTION CODE
Approved for public release; distribution is unlimited.	*A

13. ABSTRACT *(maximum 200 words)*

The Janus combat simulation offers the user a wide variety of weather effects options to employ during the execution of any simulation run, which can directly influence detection of opposing forces. Realistic weather effects are required if the simulation is to accurately reproduce "real world" results. This thesis examines the mathematics of the Janus Weather Effects Models. A weather effect option in Janus is the Sky-to-Ground Brightness Ratio (SGR). SGR affects an optical sensors ability to detect targets. It is a measure of the sun angle in relation to the horizon. A review of the derivation of SGR is performed and an analysis of SGR's affect on the number of optical detections and detection ranges is performed using an unmanned aerial vehicle (UAV) search scenario. For comparison, the UAVs are equipped with a combination of optical and thermal sensors.

14. SUBJECT TERMS Weather effects, Detection, XSCALE, Optical, Janus, Unmanned aerial vehicle, Sky-to-ground brightness ratio.	15. NUMBER OF PAGES 80
	16. PRICE CODE

17. SECURITY CLASSIFICATION OF REPORT	18. SECURITY CLASSIFICATION OF THIS PAGE	19. SECURITY CLASSIFICATION OF ABSTRACT	20. LIMITATION OF ABSTRACT
Unclassified	Unclassified	Unclassified	UL

NSN 7540-01-280-5500

Standard Form 298 (Rev. 2-89)

Prescribed by ANSI Std. 239-18 298-102

Approved for public release; distribution is unlimited.

A MATHEMATICAL ANALYSIS OF THE JANUS COMBAT SIMULATION WEATHER EFFECTS MODELS AND SENSITIVITY ANALYSIS OF SKY-TO-GROUND BRIGHTNESS RATIO ON TARGET DETECTION

by

Vincient F. Shorts
Lieutenant Commander, United States Navy
B.S., United States Naval Academy, 1980

Submitted in partial fulfillment
of the requirements for the degree of

MASTER OF SCIENCE IN APPLIED MATHEMATICS

from the

NAVAL POSTGRADUATE SCHOOL
September 1994

Author: [redacted]
Vincient F. Shorts

Approved by: [redacted]
Bard Mansager, Thesis Co-Advisor

[redacted]
Maurice Weir, Thesis Co-Advisor

[redacted]
R. Franke, Chairman
Department of Mathematics

ABSTRACT

The Janus combat simulation offers the user a wide variety of weather effects options to employ during the execution of any simulation run, which can directly influence detection of opposing forces. Realistic weather effects are required if the simulation is to accurately reproduce "real world" results. This thesis examines the mathematics of the Janus Weather Effects Models. A weather effect option in Janus is the Sky-to-Ground Brightness Ratio (SGR). SGR affects an optical sensors ability to detect targets. It is a measure of the sun angle in relation to the horizon. A review of the derivation of SGR is performed and an analysis of SGR's affect on the number of optical detections and detection ranges is performed using an unmanned aerial vehicle (UAV) search scenario. For comparison, the UAVs are equipped with a combination of optical and thermal sensors.

TABLE OF CONTENTS

LIST OF TABLES

LIST OF FIGURES

I. INTRODUCTION

A. BACKGROUND

1. The Janus Combat Simulation

There are many types of combat simulations in use today. Some of these combat models simulate conflicts on a global scale, where the principal opposing forces are nations or alliances. These types of simulations are referred to as low resolution models. There are also theater level simulations which model specific areas of operations, such as the Persian Gulf. The Janus Combat Simulation, named for the two-faced Roman god who was the guardian of portals and the patron of beginnings and endings, models conflicts on a much smaller scale. Janus models conflict at the unit level, such as squad, company or battalion sized elements. Janus is classified as a high resolution simulation model.

Janus currently exists in several versions. It was initially a nuclear effects simulation developed by the Lawrence Livermore National Laboratory. This version, known as Janus(L), was also used for limited tactical training by the Army. The Army Training and Doctrine Command (TRADOC) and TRADOC Analysis Command (TRAC) then initiated Janus(T) for army combat systems development needs. A refinement of Janus(T), whose objective was to satisfy both the combat

development needs and the tactical training requirements, is Janus Army, or Janus(A). This version will be referred to as simply "Janus" throughout the remainder of this thesis (Janus Users Manual, 1994). If combat simulations are to have real utility, they must be able to represent the "real world" to a high degree of accuracy. Some simplifications are required to make the simulation manageable. The need to model environmental conditions realistically is critical, since most wars are fought on not just clear days and nights nor under perfect weather conditions.

a. Characteristics

Janus is an interactive, two-sided, closed, stochastic, ground combat simulation model presented with precise color graphics (Janus Users Manual, 1994).

- *Interactive* refers to the interplay of opposing force commanders or a single analyst who can make key decisions during crucial situations while the simulation is in progress. The ability to call in artillery support, or to mount or dismount troops provide simple examples of the interaction possibilities.

- *Two-sided* refers to two opposing forces; a Blue Force and a Red Force. These forces can be directed simultaneously by two sets of players, or on the UNIX-based version by a single analyst running two windows.

- *Closed*, for the two commander version, means that the disposition of opposing forces is largely unknown.

- *Stochastic* refers to how the simulation determines actions and their results. A stochastic process is governed by the laws of probability and chance. So, results of actions are based on probabilities of detection, hit, kill, etc.

- *Ground combat* means that the principal focus of Janus is on ground maneuver units.(However it is capable of simulating air and sea maneuvers to a limited degree.)

b. Terrain Representation

Janus uses digitized terrain representations developed by the Defense Mapping Agency. The terrain is displayed in a form familiar to military users with contour lines, roads, rivers, vegetation, and urban areas. Contour lines are displayed in the color grey, streams and bodies of water in blue, roads and urban areas in yellow, and vegetation in green. Realistically, the terrain affects visibility and movement of forces by influencing the lines of sight and rates of movement. A mechanized force would not be able to move through a dense forest area at maximum speed of advance, for example or be able to "acquire" or see targets at maximum range through foliage.

c. Simulation Realism

Janus attempts to model accurately Blue and Red weapon systems as a function of each system's predicted capabilities as affected by terrain and weather. The user must consider all factors which influence the combat capability of these forces just as would be the case in an actual engagement. If, for example, a commander wishes to employ helicopters to suppress enemy armor when the cloud ceiling is below the helicopter altitude, then the suppression mission must have a

very low probability of success. Just as with any actual mission, Janus planners who consider all military factors and begin with tactically sound plans will receive superior training.

d. Post-simulation Review and Analysis

Janus offers an excellent capability for post-simulation review and analysis of engagements. Engagement results are available in two ways. First, the Janus workstation can replay the entire engagement exactly as it ran during the simulation. Second it allows the user to retrieve and display graphically simulation results, like time and location of direct fire kills. The simulation post-processor files display engagement reports either on the screen or in printed form.

e. Additional Features

Janus offers other features such as Multiple Runs with Branchpoints (caused by the force commander choosing a different course of action at a particular point in the scenario), AUTOJAN Replay and Data Base options which can be found in the user's manual.

2. Environmental Effects

Janus has the capability of defining up to 16 different weather options or conditions. The user can specify the basic weather characteristics that will be used by Janus during the execution of the simulation . Chapter II details

the contribution made by each of the following parameters (Janus Users Manual, 1994):

- *Visibility* (in meters) - establishes the maximum horizontal range for optical sensors. No system can acquire targets optically at ranges greater than the distance entered.
- *Wind Direction* - establishes the wind direction and affects the movement direction of smoke, dust and chemical clouds.
- *Wind Velocity* - establishes wind speed and affects the speed of dust, smoke and chemical clouds.
- *EOSAEL XSCALE Atmospheric Model* (1-4) - establishes which of several atmospheric models are actually used by Janus. This parameter affects target detection and acquisition range.
- *Air Mass Type* (1=maritime arctic,2=maritime polar, 3=continental polar) - selects which of several air mass models are used. This parameter also affects target detection and acquisition range.
- *Ceiling* - establishes the cloud ceiling used by Janus and affects detections, especially for aircraft.
- *Relative Humidity* - affects smoke, dust, and chemical clouds used in the simulation. Factors into account the XSCALE atmospheric model which affects detection.
- *Temperature* - establishes the ambient temperature used in the simulation.
- *Inversion Factor*(0-5) - affects smoke, dust, and chemical cloud growth.
- *Extinction Coefficient Band 1-2* - for the optical spectral band entered in units of 1 per kilometer (1/Km), this parameter affects the rapidity with which visual acuity is lost.
- *Extinction Coefficient Band 3-4* - for thermal sensors in the seven to thirteen micron spectral band, this parameter affects the performance of thermal sensors.
- *Optical Contrast* - The target-to-background brightness ratio. Janus assumes a constant optical contrast of all

targets. This parameter only affects the performance of optical sensors.

- *Sun Angle* - Not currently modeled. If this parameter is modeled it would allow the play of a "sun in the eyes" vs "sun at back" scenario.

- *Sky-to Ground Brightness Ratio* - the location of the sun in relation to the target and the ground, this parameter affects the performance of optical sensors.

A typical Weather Data Entry Screen is shown in Figure (1).

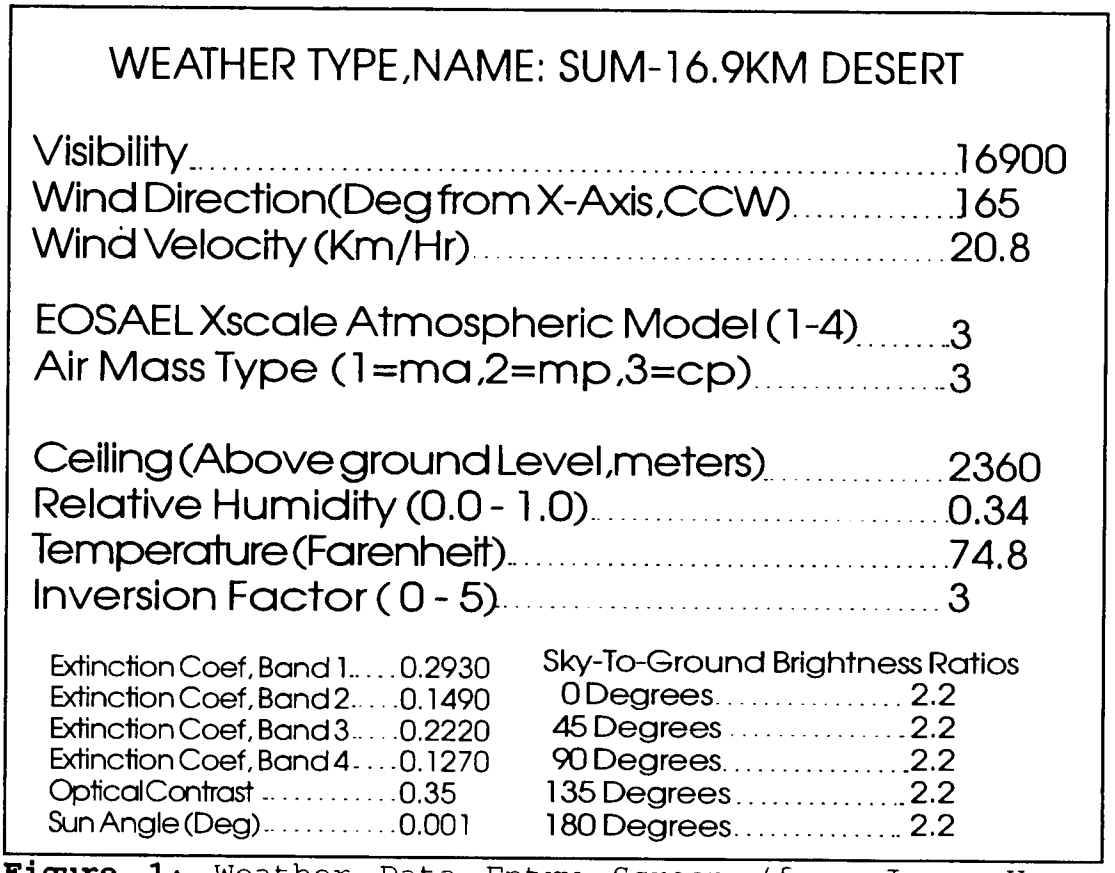

Figure 1: Weather Data Entry Screen (from Janus Users Manual, 1994)

B. STATEMENT OF THESIS

The ability to acquire a target is the crucial element in the success or failure of a combat engagement. Janus models weather effects, which can play a major role in the acquisition results and directly affect the fire kill results, and these effects should be portrayed in any realistic simulation.

The Janus combat simulation offers the user a wide variety of weather effects options to employ during a particular simulation run. Each option can directly influence detection of the opposing forces. However, the vast majority of users completely ignore the options available, mainly due to inadequate documentation on their usage. Thus most Janus scenarios are simply executed on a clear day or night with little impediment to visibility. This thesis explains how weather effects and detection criteria are modeled in Janus and how they can be utilized effectively. We also perform a sensitivity analysis of the Sky-to-Ground Brightness Ratio, which can affect optical sensor detections, using a search scenario with Unmanned Aerial Vehicles (UAV) equipped with optical and thermal sensors. A by-product of this study is a "Weather Tutorial", which helps potential users improve the fidelity of their combat simulations.

II. ACQUISITION AND WEATHER EFFECTS MODELS

A. ACQUISITION MODEL

The phases in the target acquisition process are detection, classification, recognition and identification.

- Detection refers to the ability to determine that an object within the field of view is or is not of military interest.
- Classification is the ability to distinguish a target by general type. For example, to classify a vehicle as tracked or wheeled.
- Recognition is the ability to discriminate between two targets of similar type.
- Identification is the ability to discriminate the exact model of a target. For example, determining a target tracked vehicle is a T-80 Tank.

This section explains, in mathematical terms, what constitutes an acquisition of a target and the mechanics by which Janus acquires a target.

1. Background Concepts

Before presenting the acquisition model it is necessary to discuss some background parameters. The following terms are needed (Hoock, 1994):

- Attenuation - the reduction of the target/background's visible signature, which is affected by meteorological visibility.
- Contrast - the visible difference between an object and its background.
- Resolvable Cycles Across Minimum Dimension of Target - the idea of resolvable cycles across a target is related to

the amount of information required to acquire and identify the target. Detection requires the fewest number of cycles and identification requires the highest number. The higher the number of cycles and the higher the contrast obtained the better the acquisition of the target, (see Figure 2).

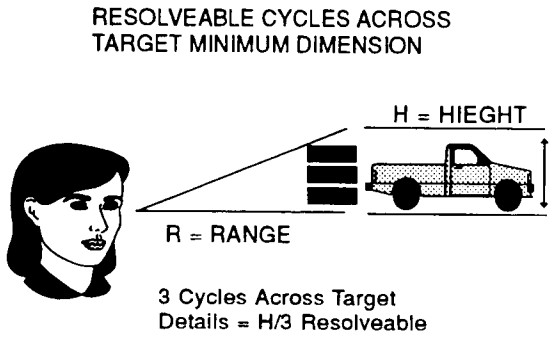

Figure 2: Resolvable Cycles (from Hoock, 1994)

- Scattering - the dispersion of the target's visible signature or its background contrast, which is usually caused by aerosols such as smoke, haze, and dust.

a. Contrast

Contrast is defined to be the visible difference between a target and its background. For instance, a black wall against a white background has a high degree of contrast, whereas a black wall against a black background has very low contrast. Contrast can also be defined in terms of a target's radiance as follows:

$$C = \frac{L_{TARGET} - L_{BACKGROUND}}{L_{BACKGROUND}}, \qquad (1)$$

where **L** is the radiance or amount of light energy given off by the object, and **C** is the object's contrast (Hoock, 1994).

b. Angular Subtense and Spatial Frequency

Angular subtense (measured in milliradians from the sensor) is the result of dividing the height of an object by its distance from the sensor (see Figure 3).

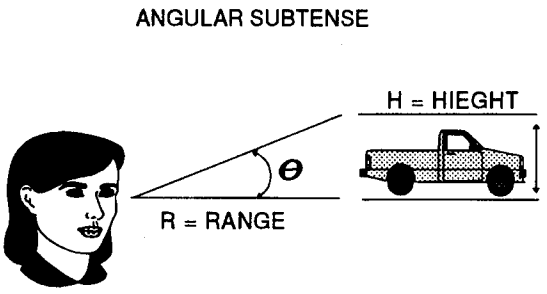

Figure 3: Angular Subtense (from Hoock, 1994)

$$\theta = \frac{H}{R}, \qquad (2)$$

where **θ** is the Angular Subtense (measured in milliradians), **R** is the range (km), and **H** is the height (m) (Hoock, 1994).

Spatial frequency is a measure of the level of detail distinguishable in the target image and is based on resolvable cycles across the target according to the formula:

$$f = \frac{cy}{\theta}. \qquad (3)$$

In Eq. (3), **cy** is the cycles across the target and **f** is the Spatial frequency (in cycles per milliradian).

Optical sensor acquisition performance or Minimum Resolvable Contrast (MRC) is based on the minimum contrast of the target/background needed by the sensor for the observer to resolve changes over a given spatial frequency (sensor range versus target height). MRC is determined by the noise and resolution limits of the sensor in question and it is significantly affected by ambient light levels. Sensor performance curves are based on ambient illumination, MRC and spatial frequency (see Figure 4).

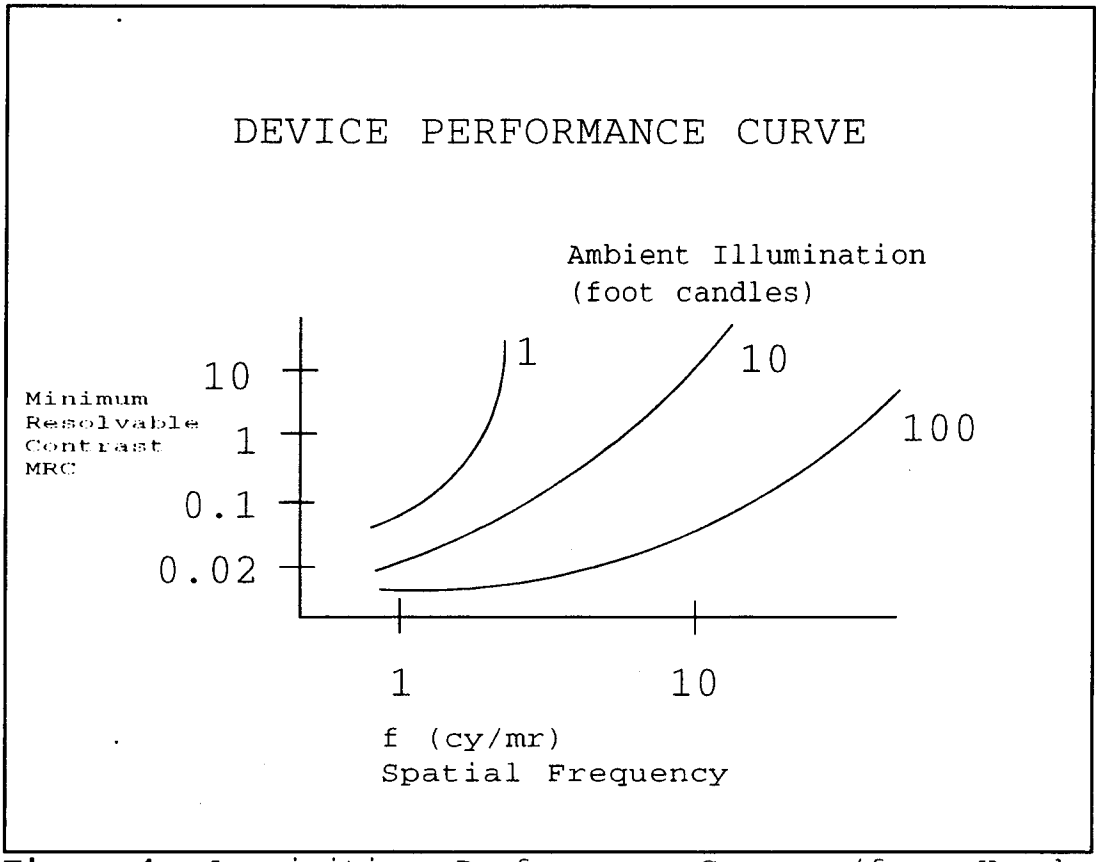

Figure 4: Acquisition Performance Curves (from Hoock, 1994)

c. Acquisition Performance

(1) The Johnson Criteria For Target Acquisition. This criteria estimates how many resolvable changes in contrast are required across a target in order to obtain a 50% probability of target acquisition. Passive target acquisition depends on both available radiance and available image resolution. The "standards" were originally determined from data collected using observers who viewed a television screen. The observers were presented bar patterns and introduced to

high frequency noise. They were then tasked to complete four steps in the acquisition process: detection, classification, recognition and identification. The Johnson test results are shown in Figure (5).

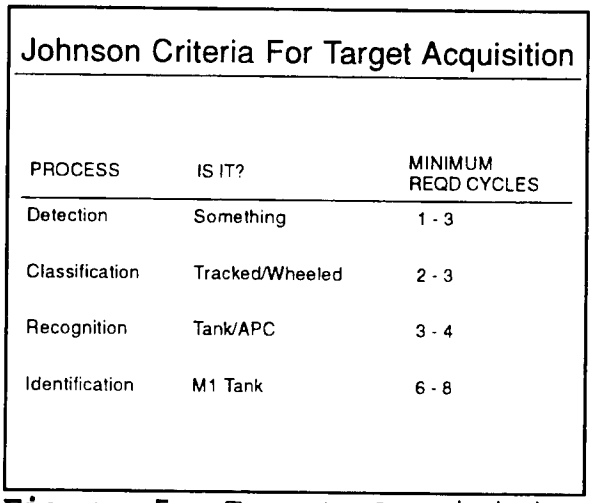

Johnson Criteria For Target Acquisition

PROCESS	IS IT?	MINIMUM REQD CYCLES
Detection	Something	1 - 3
Classification	Tracked/Wheeled	2 - 3
Recognition	Tank/APC	3 - 4
Identification	M1 Tank	6 - 8

Figure 5: Target Acquisition Criteria (from Hoock, 1994)

The tests revealed that up to three times the number of cycles were required for each step of acquisition when additional high frequency noise was introduced as clutter. For a signal-to-noise ratio of 2.8 - 3.2, zero clutter typically required 1 cycle for detection, but as clutter was increasingly introduced 1 - 3 cycles were needed (Hoock, 1994).

(2) Direct Transmittance. A primary factor affecting visual target acquisition is the target's energy ability to penetrate its surroundings which affects how well

the image is transmitted to the receiver. An image received by the optical receptors passes through the surrounding environment, a process which is known as atmospheric transmittance.

- Molecular transmittance has its smallest values at the higher temperature and humidities, especially in the mid and far infrared bands.
- Aerosol transmittance is defined by the penetration of natural phenomena like clouds, fog, haze etc.
- Smoke-and-dust transmittance are self-explanatory (whether effects are man-made or natural).

The total atmospheric transmittance, **T** for a particular wavelength, is the product of each component value (Hoock, 1994):

$$T = T_{MOLECULAR} \cdot T_{AEROSOL} \cdot T_{SMOKE} \cdot T_{DUST} \cdot$$

2. Janus Target Acquisition

Figure (6) displays the NVEOL acquisition algorithm used in Janus which we now discuss.

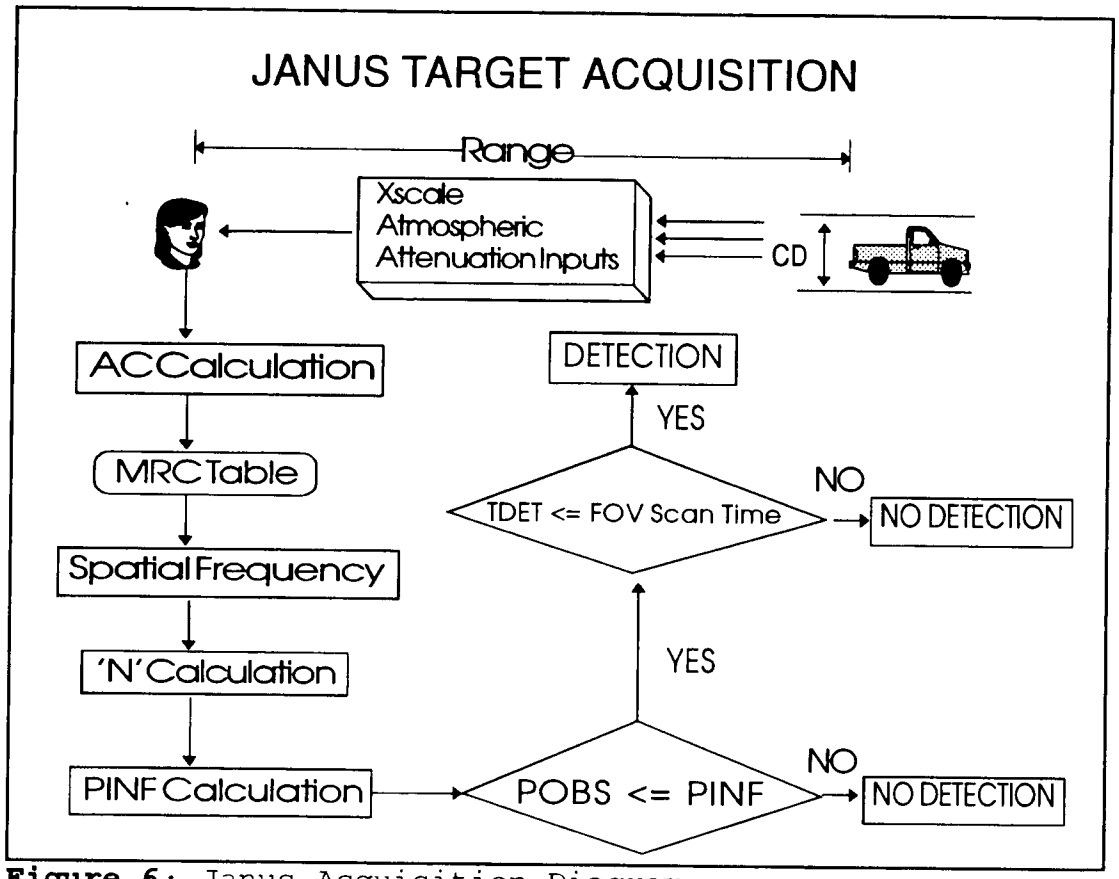

Figure 6: Janus Acquisition Diagram

The target acquisition algorithm begins with the sensor's range from target and the atmospheric conditions. The target contributes its critical dimension (**CD**), which is the minimum observable dimension, and its intrinsic contrast (**IC**) which is the contrast of the object unaffected by any attenuation. Janus calculates the apparent contrast (**AC**) which is contrast degraded by atmospheric attenuation, according to the formula:

$$AC = \frac{IC}{1.0 + \exp[\,-\,(AT \cdot R)\;-1.0]}, \qquad \textbf{(4)}$$

In Eq. (4), (**AT**) is the attenuation effects and (**R**) is range. **AT** values are available for the environmental conditions present.

The MRC Tables are entered and the **AC** calculation is used to find the Spatial Frequency (in number of cycles per milliradian). To illustrate, suppose we wanted to know the spatial frequency for the unmagnified eye in clear weather under daylight conditions and the calculated value returned for **AC** was 0.350. Table I would be entered with the contrast value of 0.35 and read across to the 1000 FL value which corresponds to a clear sunlight day. The value of 1.726 CY/MR would then be used for spatial frequency.

Table I: Contrast vs Cycles Per Milliradian

MINIMUM RESOLVABLE CONTRAST

Contrast vs Cycles Per Milliradian
Eye 100% Transmittance-Magnification=1

CONTR	1000FL CY/MR	100FL CY/MR	10FL CY/MR	1FL CY/MR	10-1FL CY/MR	10-2FL CY/MR	10-3FL CY/MR	10-4FL CY/MR
0.02	0.000	0.000	0.000	0.000	0.000	0.000	0.000	0.000
0.03	0.650	0.601	0.470	0.275	0.000	0.000	0.000	0.000
0.04	0.810	0.760	0.624	0.429	0.174	0.000	0.000	0.000
0.05	0.914	0.863	0.723	0.523	0.265	0.000	0.000	0.000
0.10	1.204	1.149	0.997	0.774	0.482	0.108	0.003	0.000
0.15	1.367	1.311	1.153	0.914	0.598	0.182	0.010	0.003
0.20	1.485	1.428	1.264	1.014	0.680	0.238	0.020	0.008
0.25	1.579	1.520	1.353	1.094	0.745	0.285	0.031	0.014
0.30	1.657	1.598	1.427	1.160	0.799	0.324	0.044	0.021
0.35	1.726	1.666	1.492	1.218	0.847	0.358	0.057	0.029
0.40	1.787	1.726	1.550	1.270	0.889	0.389	0.071	0.037
0.45	1.842	1.781	1.602	1.317	0.927	0.417	0.085	0.046
0.50	1.893	1.813	1.652	1.361	0.923	0.443	0.099	0.055
0.55	1.941	1.879	1.696	1.401	0.996	0.467	0.113	0.064
0.60	1.986	1.924	1.739	1.440	1.027	0.491	0.126	0.073
0.65	2.029	1.996	1.780	1.467	1.057	0.512	0.140	0.082
0.70	2.071	2.007	1.819	1.511	1.086	0.533	0.153	0.091
0.80	2.150	2.085	1.894	1.579	1.140	0.573	0.179	1.180
0.90	2.226	2.160	1.966	1.643	1.093	0.612	0.204	1.126

NOTES: This data is transcribed the from the Janus User's Manual.

(10^{-5}) foot lamberts is equivalent to Starlight, No Moon.

(10^{-4}) foot lamberts is equivalent to Quarter Moon Sky.

(10^{-3}) foot lamberts is equivalent to Lower Civil Twilight.

(10^{-2}) foot lamberts is equivalent to Upper Civil Twilight.

1 FL is equivalent to Just Prior to Sunrise/After Sunset.

10 FL is equivalent to Very Heavily Overcast Day.

100 FL is equivalent to Lightly Overcast Day.

1000 FL is equivalent to Clear Sunlight Day.

Next Janus calculates **N** (the number of cycles required to detect the target):

$$N = \frac{f \cdot CD}{R}, \qquad (5)$$

where **f** is the Spatial Frequency obtained from Table I. Janus then calculates the probability of acquiring the target given an infinite amount of time (**PINF**):

$$PINF = \frac{\left[\frac{N}{N50}\right]^{(2.7 + (0.7 \cdot [\frac{N}{N50}]))}}{1.0 + \left[\frac{N}{N50}\right]^{(2.7 + (0.7 \cdot [\frac{N}{N50}]))}}, \qquad (6)$$

In Eq. (6), **N50** is the number of resolvable cycles that must be present for the average observer's required level of detection for weapons release in Janus (i.e. detection, aimpoint or recognition). Equation (6) is formulated so that the largest value for **PINF** is 0.5. If **N** is small with respect to **N50** then **PINF** is also small. The smaller the **PINF** value is, the smaller is the prospect for detection, as shown below.

During a battle, a random number (**POBS**) with a uniform [0,1] probability distribution is drawn once for each observer's sensor. If $POBS \leq PINF$ a detection may take place and Janus draws another uniform [0,1]-random number (**PD**) for the observer for a field of view (FOV) scan. The number **PD** is

used to find the target detection time, (**TDET**) according to the formula:

$$TDET = \frac{3.4}{PINF} \times [\ln(1.0 - \frac{PD}{PINF})]. \qquad (7)$$

If **TDET** is less than or equal to the FOV scan time a detection occurs, otherwise no detection occurs (NVEOL, 1994).

B. JANUS WEATHER EFFECTS MODELS

1. XSCALE Model

We will now examine the XSCALE atmospheric attenuation inputs referred to in Figure (6). One of the main sources used today for weather effects simulation models is the Electro-Optical Systems Atmospheric Effects Library (EOSAEL). Janus uses the EOSAEL model XSCALE to simulate optical attenuation by natural atmospheric aerosols (haze and fog), rain, snow and low clouds. XSCALE assumes that the aerosols are horizontally homogeneous. This allows the use of Beer's law (which states that the horizontal transmittance at a particular wavelength and range is exponentially related to the range and the wavelength extinction coefficient) to calculate the horizontal transmittance:

$$T_\lambda(R) = \exp(-K_\lambda \cdot R), \qquad (8)$$

In Eq. (8), **K** is the extinction coefficient (a measure of the rate of loss of visual acuity in a particular medium), **λ** the wavelength, and **R** the range. The range of wavelengths modeled by XSCALE is $0.2\mu m < \lambda < 12.5\mu m$, which is well into the infrared bandwidth (Fiegel, 1994).

XSCALE models both the horizontal and the slant angle lines of sight, Each of these are discussed separately.

a. Aerosol Attenuation Along Horizontal Paths

A theoretical model of the aerosols (Haze) of the lower atmosphere (Shettle and Fenn, 1979) is used to calculate extinction and absorption coefficients for maritime, rural and urban aerosols, i.e. the different types of haze, controlled in Janus by selection of Air Mass Type. The model assumes a bimodal, lognormal particle size distribution of the form:

$$\frac{dn(r)}{dr} = \sum_{i=1}^{2} \frac{N_i}{\ln(10) \cdot \sqrt{2\pi} \cdot r \cdot \sigma_i} \exp -\left[\frac{(\log r - \log r_i)^2}{2(\sigma_i)^2}\right], \quad (9)$$

where $\mathbf{r_i}$ is the mode radius of mode **i**, $\mathbf{N_i}$ is the number density associated with $\mathbf{r_i}$, and σ_i is the standard deviation for mode **i**. The bimodal assumption implies there is a partition of the particle size distribution into two groups with different mode radii. The mode of a distribution is most frequently occurring value.

The particle distribution is a function of the air mass point of origin and the relative humidity. Based on the

work of Hanel (Hanel, 1976), atmospheric particles grow with increasing relative humidity. Using *dn/dr* of Eq. (9) and the refractive indices of the particular air mass model, Shettle and Fenn (Shettle and Fenn, 1979) used standard Mie theory[1] to calculate extinction and absorption coefficients for each air mass haze at 8 relative humidities (0,50,70,80,90,95,98, and 99 percent) and at 31 wavelengths (in the 0.2μm - 12.5μm range) for each humidity, and tabulated the results . XSCALE utilizes the tabulated results as look-up tables, normalized to the 0.55μm extinction coefficient at each humidity. To scale the results to any visibility, XSCALE uses the empirical Koschmieder relation:

$$K_{0.55} = \frac{3.912}{V}, \qquad (10)$$

to determine the extinction coefficient $\mathbf{K}_{0.55}$ for the visibility (**V**). The value 3.912 corresponds to a 2 percent contrast threshold, the distance over which the contrast of a target drops by 98 percent (Fiegel, 1994).

To find coefficients for arbitrary values of relative humidity and wavelengths, XSCALE takes input values of

[1] Mie theory calculates the scattering and absorption of an incident plane electromagnetic wave by a single spherical particle. In order to determine the attenuation of a collection of particles, Mie calculations are performed for each type and size particle, then summed over the particle distribution. (Bohren and Huffman, 1983)

relative humidity, visibility, and wavelength and performs linear interpolation between wavelengths and logarithmic interpolation between relative humidities. The Army Research Lab, Battlefield Environment Directorate has conducted field tests to measure particle size distributions under low visibility conditions (Lindberg, 1982; Lindberg, 1984; Lindberg and others, 1984). Data from these field tests have been compared with theoretical air mass particle size predictions. The overall agreement with these test results justifies the use of the model to predict horizontal extinction and absorption coefficients of the lower atmosphere.

(1) Fog Models. The range of fogs in nature are represented by two models in XSCALE (Fiegel, 1994). The models are again Mie calculations based on the particle size distribution and XSCALE identifies them as fog-one (typical advection)and fog-two (radiation). These fogs have particle size distributions represented by Deirmendjian's modified gamma distribution (Deirmendjian, 1964):

$$\frac{dn}{dr} = Ar^{\alpha} \exp(-br) . \qquad (11)$$

For fog-one Eq. (11) becomes:

$$\frac{dn}{dr} = 0.06592r^3 \exp(-0.3r). \qquad (12)$$

For fog-two Eq. (11) becomes:

$$\frac{dn}{dr} = 607.5r^6 \exp(-3r). \qquad (13)$$

The gamma distribution is a good model for particle size since it models non-negative random variables which are skewed to the right, with most of the area under the density function near the origin and the density function dropping gradually as you move away from the origin. Fog particle sizes are non-negative, and the number of particles decreases as particle size increases.

The fog models are implemented in the same fashion as the haze models discussed previously. The values have been tabulated for 31 wavelengths but only at 100 percent relative humidity. As in the haze model, XSCALE interpolates for intermediate values (Fiegel, 1994).

(2) Rain Models. XSCALE uses Mie theory to calculate the attenuation in the visible and infrared due to raindrops. The model expresses attenuation as a function of rain rate. Visible and infrared wavelengths are much smaller than the radius of most raindrops, which typically range from $50\mu m$ to a few millimeters. To eliminate the wavelength

dependence of the extinction coefficient in the 0.2 - 12.5μm band, XSCALE assumes a Mie extinction coefficient of 2. The resulting extinction coefficient for rain is then:

$$K = 2\pi \int N(r)\ r^2\ dr, \qquad (14)$$

where **N(r)** is the rain particle size distribution and **r** is the radius of the raindrop.

Considerable work has been done on raindrop size distribution models. XSCALE uses the results of Waldvogel (Waldvogel, 1974) to represent drizzle, widespread rain and thunderstorm size distributions. The general form of the raindrop size distribution is:

$$N(d) = N_0 \exp(-\Lambda d), \qquad (15)$$

where $\Lambda = 4.1R^{-0.21}\ (mm^{-1})$, $N_0 = 8 \times 10^3\ (m^{-3}\ mm^{-1})$, **d** is the droplet diameter and **R** is the rain rate (mm/h). XSCALE uses the following to calculate extinction coefficients:

$$K = 0.5089\ R^{0.63} \quad drizzle, \qquad (16)$$

$$K = 0.3201\ R^{0.63} \quad widespread\ rain, \qquad (17)$$

$$K = 0.1635\ R^{0.63} \quad \textit{thunderstorm.} \qquad (18)$$

Equation (17) is recommended for general use and is the default in XSCALE if a specific model is not requested. The user can simulate a thunderstorm or drizzle by calculating the proper extinction coefficients and entering values in the optical bands on the weather data entry page in Janus.

(3) Falling Snow Model. XSCALE defines falling snow as,

> Precipitating snow carried by a wind of less than 5 m/s and a relative humidity of less than 95 percent.

Falling snow is relatively large (100μm or more) in comparison with visible and infrared wavelengths. However, field measurements of transmittance have shown that there does exist a dependence upon wavelength in falling snow such that the extinction coefficient increases with wavelength in the absence of coexisting fog (Fiegel, 1994). This spectral dependence can be explained for the most part by considering diffraction effects. Fiegel explains it as follows:

> The forward direction diffraction is very narrow at visible wavelengths, but increases in width with wavelength. Thus, less diffracted energy is directed along the line of sight to enter the transmissometer as the wavelength increases, resulting in an increasing extinction coefficient with wavelength. (Fiegel, 1994)

Seagravès (Seagraves,1984) used the diffracted energy entering a detector to make an approximation to calculate the radiative transfer in snow and give the functional dependence of the

spectral variations in extinction on path length **P**, detector radius $\mathbf{r_d}$, and snow particle size $\bar{r}$:

$$\frac{K(\lambda_1)}{K(\lambda_2)} = \frac{\exp(-0.88C(\lambda_1)) + 1}{\exp(-0.88C(\lambda_2)) + 1}, \qquad (19)$$

In Eq. (19), the subscripts indicate values corresponding to two different wavelengths, path lengths, detector radii, or particle size. The C_{λ_i} are given by:

$$C(\lambda_i) = 2\pi\bar{r}\frac{r_{d_i}}{\lambda_i P_i}. \qquad (20)$$

XSCALE estimates $\bar{r}$ by assuming it to be a function of surface temperature $\mathbf{T^o}$ (based on the observation that warmer snow fall is generally larger in size):

$$\bar{r} = 100\mu m \quad T^0 \le -15C, \qquad (21)$$

$$\bar{r} = (250 + 10T^0)\,\mu m \quad -15C \le T^0 \le 0C, \qquad (22)$$

$$\bar{r} = (250 + 25T^0)\,\mu m \quad -0C \le T^0 \le 2C, \qquad (23)$$

$$\bar{r} = 300\mu m \quad T^0 > 2C. \qquad (24)$$

The extinction coefficient $K(\lambda)$ used by XSCALE at wavelength λ as a function of visibility **V** is obtained from Eq. (19) with $\mathbf{r_d}$ and **P** fixed:

$$K(\lambda) = \frac{\exp(-0.88C(\lambda)) + 1}{\exp(-0.88C(0.55\mu m)) + 1} \cdot \frac{3.912}{V}. \qquad (25)$$

Note: XSCALE models blowing snow in much the same fashion.

(4) Snow and Fog. Modeling attenuation through snow and fog is accomplished by using a combination of the snow and fog extinction coefficients. If **B** ($0 \leq B \leq 1$) is the fraction of the total extinction due to snow, then

$$K(\lambda) = (1-B)K_{F\lambda} + BK_{S\lambda}. \qquad (26)$$

b. Inclined Lines of Sight Models

Janus does not use the previously described models in XSCALE to calculate horizontal extinction coefficients. The values for each band are entered on the weather data entry page. However it was necessary to understand those concepts because Janus does use XSCALE to calculate the extinction coefficients for inclined lines of sight using the horizontal models as a basis for the inclined calculations.

The large scale employment of precision guided munitions and sophisticated electro-optical sensors has increased the emphasis on near the surface visibility at inclined lines of sight (slant paths). When modeling slant path visibility, changes in the vertical and horizontal conditions must both be considered. A large number of observations have shown that the measured visibility at the surface can be significantly different from the visibility a

few hundred or so meters above the surface(Fiegel, 1994). Therefore, slant path visibility may be radically different from horizontal visibility. Heaps discovered that in a significant number of cases, visibility is degraded with increased height above the surface.

The extinction and absorption tables for hazes and fogs previously described, along with semi-empirical formulae for visible extinction and relative humidity profiles are used to predict extinction as a function of height. Low-lying clouds are modeled using fog-one particle size distributions.

The transmittance along a path of varying extinction is obtained from Eq. (8) by using the average extinction coefficient along the path. Figure 7 shows the geometry of slant path.

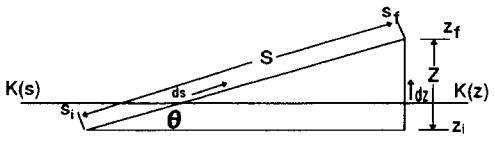

Figure 7: Slant Path Geometry
(from Fiegel, 1994)

The average extinction is the path integral divided by the path length:

$$\overline{K} = \frac{1}{S} \int_{s_i}^{s_f} K(s)\, ds, \qquad (27)$$

In Eq. (27), **S** represents the spatial path, which is the distance between the initial and final points, $\mathbf{S = s_f - s_i}$. The variable **Z** in Figure (7) is the vertical displacement of the path, (so $\mathbf{Z = z_f - z_i}$), and $\boldsymbol{\theta}$ is the elevation angle. Thus **ds** can be written as $ds = \frac{dz}{\sin\theta} = \frac{S\, dz}{Z}$. The value of **K** depends only on altitude, with **K(s) = K(z)** in the horizontal, as shown in Figure (7). Therefore $\overline{K}$ can be expressed in terms of altitude, as follows:

$$\overline{K} = \frac{1}{S}\frac{S}{Z}\int_{z_i}^{z_f} K(z)\, dz = \frac{1}{Z}\int_{z_i}^{z_f} K(z)\, dz. \qquad (28)$$

XSCALE approximates this integration by the finite sum

$$\overline{K} = \frac{1}{Z} \sum_{i=1}^{N-1} \frac{K_i + K_{i+1}}{2} \cdot (z_{i+1} - z_i), \qquad (29)$$

for **N** points along the path (Fiegel, 1994).

XSCALE uses four different models to predict a vertical extinction profile, giving rise to the choice of

atmospheric models 1 - 4 on the weather data entry screen in Janus. These models are identified as follows:

- Model 1: Used for dense fogs at ground level or when one is at the cloud base or in a cloud. Physically this model represents the increase in liquid water content resulting in decreased visibility due to an increasing extinction coefficient of a saturated parcel of air rising at the wet adiabatic lapse rate (Heaps, 1983; Fiegel, 1994).

- Model 2: Used for visibility conditions ranging from clear-to-hazy-to-light fog when there is a low cloud ceiling present (Fiegel,1994).

- Model 3: Used when a shallow radiation fog is present or when a haze layer is capped by a distinct low lying temperature inversion. No cloud ceiling is present (Fiegel,1994).

- Model 4: Used for regions of reasonable vertical homogeneity of visibility in a clear to slightly hazy atmosphere that may have a shallow haze layer near the surface. No cloud ceiling is present (Fiegel,1994).

Figure (8) summarizes models 1 through 4 with associated regions and affects on the extinction coefficient and visibility.

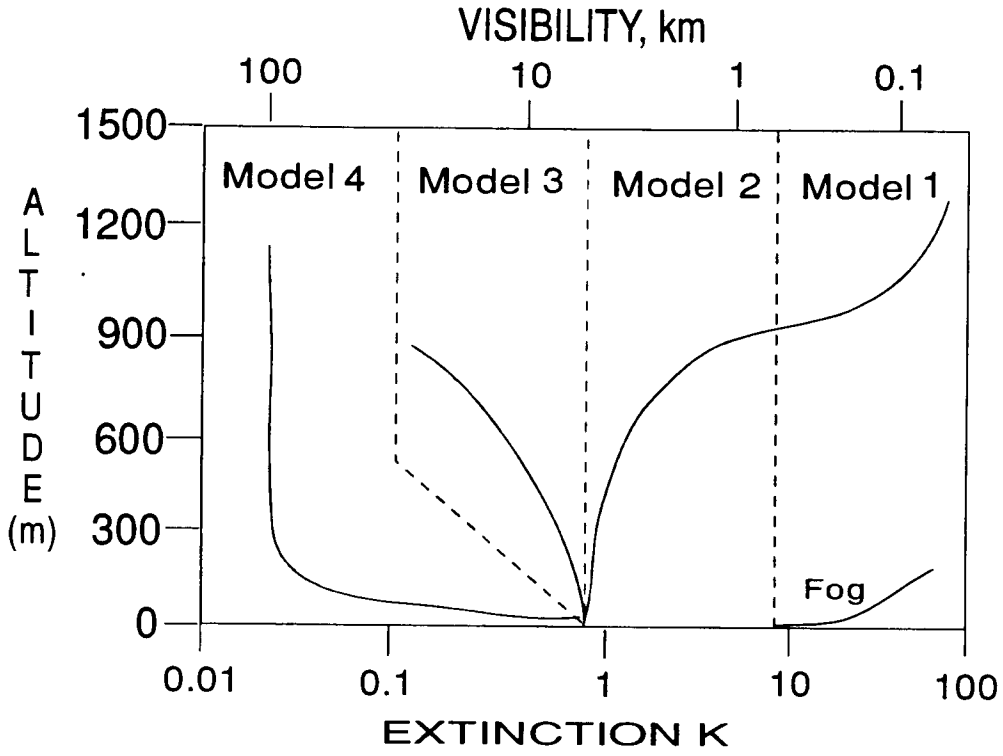

Figure 8: Vertical Structure Models

2. Inversion Factor Model

An inversion height is the height above which the temperature ceases to increase with increased height (JTCG/ME, 1990). When an inversion exists (usually at night), the mixing height is taken to be the base of the inversion. Below the mixing height, turbulence caused by wind, heat flux or eddy diffusion keeps the air well-stirred or mixed. The inversion layer acts as a more or less impermeable barrier that tends to confine an obscurant cloud, like smoke or dust.

The inversion factor model in Janus is based on the Pasquill Stability Categories (PSC) method (JTCG/ME,1990).

The PSC method ranks stability into six broad categories. Table II shows the PSC categories and their Janus equivalent.

Table II: Janus Inversion Factor

INVERSION FACTOR MODEL

PSC Category	Janus Inversion Factor	Condition
A	0	Extremely Unstable
B	1	Moderately Unstable
C	2	Slightly Unstable
D	3	Neutral
E	4	Slightly Stable
F	5	Moderately Stable

Unstable conditions (Categories 0 - 2) generally imply high levels of turbulence and air temperatures that decrease with height. Stable conditions (Categories 4 - 5) generally imply low levels of turbulence associated with an inversion condition. Unstable conditions prevail during the day whereas stable conditions tend to prevail at night. Neutral conditions (Category 3) can occur during either day or night times.

As mentioned previously, the inversion factor primarily affects the formation and behavior of smoke and dust clouds.

3. Sky-to-Ground Ratio

The sky-to-ground brightness ratio (SGR) models the contrast loss in direct view optics due to the effects of ambient light. The ratio SGR varies with sun angle: the lower the sun angle, the greater is the SGR value. A higher SGR means target contrast is lost due to a "sun in the eyes" effect. Janus does not vary the sun angles and uses an average value of SGR for the simulation. Thus, Janus cannot truly play a "sun in eyes" scenario. Also, even though Janus enters values for SGR every 45 degrees, only the zero bearing is modeled currently.

a. Deriving the Sky-to-Ground Ratio

Recall (from Chapter II, page 10) that **L** is the radiance, **T** the transmittance and **C** the contrast. The radiance of a target at some arbitrary position **s**, is dependent upon the radiance at the target's initial location, $\mathbf{L_{targ}(0)}$, with degradation due to transmission losses and path radiance influences (Hoock, 1994). Formally,

$$L_{targ}(s) = L_{targ}(0) \cdot T(s) + L_{path}. \qquad (30)$$

Likewise, the radiance of the background at some position **s** is:

$$L_{back}(s) = L_{back}(0) \cdot T(s) + L_{path}(s). \qquad (31)$$

From Eq. (1) the target contrast at **s** is:

$$C(s) = \frac{L_{targ}(s) - L_{back}(s)}{L_{back}(s)}. \qquad (32)$$

Substituting Eq. (30) and (31) into Eq. (32) yields:

$$C(s) = \frac{[L_{targ}(0) - L_{back}(0)] \cdot T(s)}{[L_{back}(0) \cdot T(s)] + L_{path}(s)}. \qquad (33)$$

Finally, dividing the denominator and numerator of Eq. (33) by **T(s)** and $\mathbf{L_{back}(0)}$ yields the result,

$$C(s) = \frac{C(0)}{1 + \frac{L_{path}(s)}{L_{back}(0) \cdot T(s)}}. \qquad (34)$$

Figure (9) summarizes the effects of the atmosphere on target images.

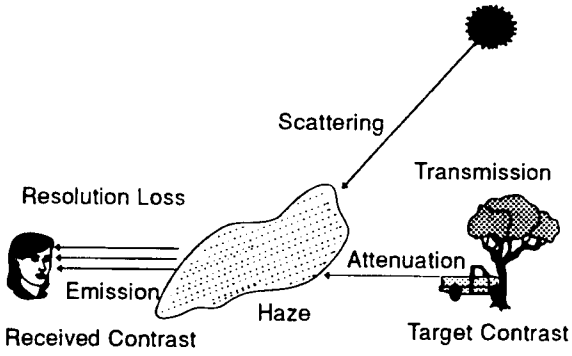

Figure 9: Atmospheric Effects on Target Images (from Hoock, 1994)

Equation (34) allows for the calculation of the contrast at some arbitrary point as a function of the initial contrast of the object and the radiance of the background, path and transmissivity (which is the ability to transmit energy through medium).

.Next we examine the radiance of the sky from an initial point to some arbitrary point (see Figure 10).

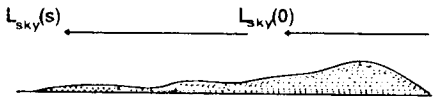

Figure 10: Radiance of Sky

For sky Eq. (30) becomes:

$$L_{sky}(s) = L_{sky}(0) \cdot T(s) + L_{path}(s). \qquad (35)$$

If we assume the radiance of the sky at some initial point is the same as the radiance at some arbitrary point, (within a localized area) then $\mathbf{L_{sky}(0) = L_{sky}(s)}$ yields

$$L_{sky} = L_{sky} \cdot T(s) + L_{path}(s), \qquad (36)$$

or

$$L_{path}(s) = [1 - T(s)]L_{sky}. \qquad (37)$$

Substituting Eq. (37) into (34) yields

$$C(s) = \frac{C(0)}{1 + \frac{L_{sky}[1 - T(s)]}{L_{back}(0)\,T(s)}} \qquad (38)$$

which simplifies to

$$C(s) = \frac{C(0)}{1 + \frac{L_{sky}}{L_{back(0)}} \cdot [\frac{1}{T(s)} - 1]}. \qquad (39)$$

The $L_{sky} \div L_{back}(0)$ factor in Eq. (39) is the SGR (Hoock, 1994), which affects the contrast of the target. As the SGR gets larger, the target contrast decreases and reduces the target's acquisition range. Similarly, as the SGR gets smaller the

target contrast is increased causing the target acquisition range to increase.

4. Summary

This chapter has described in considerable mathematical detail the models used by Janus to provide the desired weather effects and target detections. For horizontal lines of sight, Janus uses input values of visibility, ceiling, air mass model, extinction coefficient and SGR to determine possible detection ranges. For inclined lines of sight, Janus employs the proper XSCALE profile and air mass models, along with inputs for the horizontal problem, to approximate the performance of optical sensors. The SGR derivation was reviewed along with simplifying assumptions made in Janus. The next chapter examines the impact of varying SGR for clear weather and fog.

III. THE EFFECTS OF SKY-TO-GROUND RATIO ON TARGET DETECTION

A. PURPOSE

This chapter investigates the effect of varying the SGR on the number and range of optical target detections in a Janus simulation.

B. BACKGROUND

1. Selecting Sky-to-Ground Brightness Ratio Values

As stated earlier, the SGR has a direct affect on the contrast loss in direct view optical sensors. In Eq. (39) recall that the term $L_{sky} \div L_{back}(0)$ is the SGR. The value of this SGR depends upon the sun elevation above the horizon, as shown in Figure (11).

Horizontal Viewing Path Toward Sun

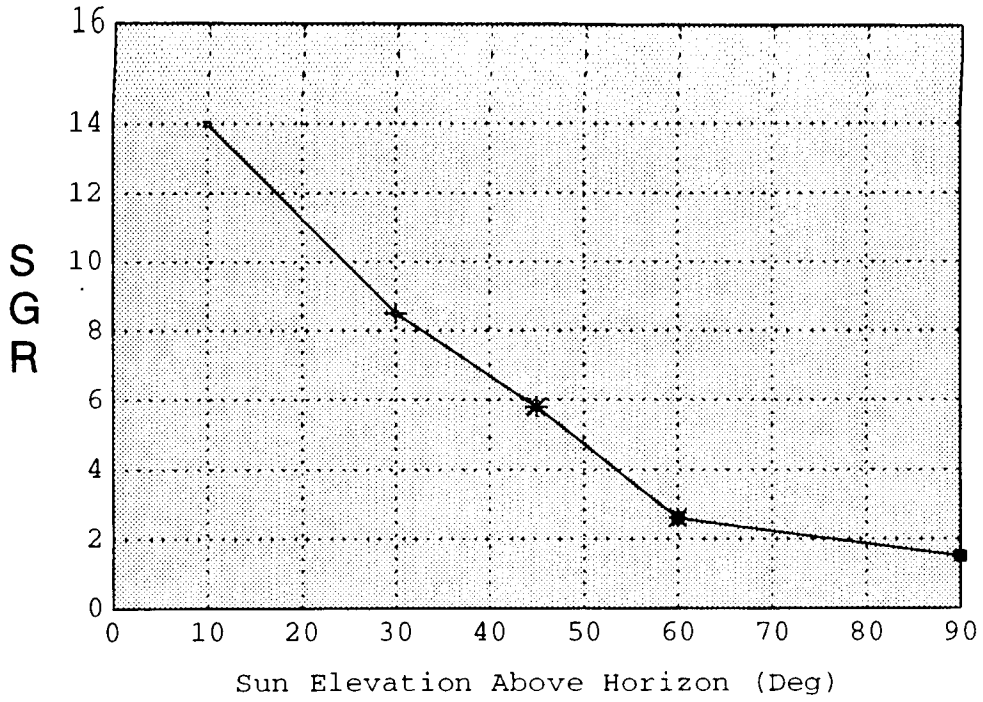

Figure 11: Sun Angle and Sky-to-Ground Ratio Relationship (Hoock, 1994)

Figure (11) also shows the three values of SGR where the slope of the graph changes significantly. These values together with the endpoints are the test values for our analysis. We need use only these values because the SGR to sun elevation relationship is piecewise linear. For instance, any results obtained between 10 and 30 degrees are linearly related. Figure (12) shows the values of SGR used in the following analysis and their representative sun angles.

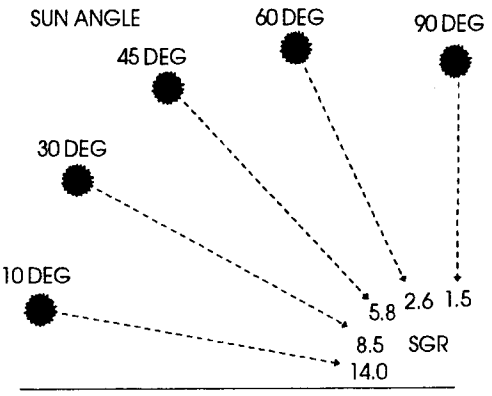

Figure 12: SGR Analysis Values

2. Infrared Comparison

Varying the SGR should have little or no effect on the performance of thermal sensors. To test this hypothesis (and ensure that changing the SGR does not completely breakdown the acquisition algorithm), thermal sensors will also be employed, to compare their detection results with the results of the optical sensors.

C. SCENARIO

1. Search Platforms

The Pioneer UAV system, operated by the U.S. Army and Navy, is used as the target acquisition platform for this scenario. The UAV can carry either a modular TV camera for daylight missions or a forward looking infrared receiver (FLIR) for day and night missions. The UAV is 14 feet long

and has a 17-foot wingspan. It weighs 450 pounds and can operate between 60 and 95 knots up to five hours at altitudes to 12000 feet. (Souter, 1994) There are two critical inputs to the scenario which are based solely on the UAV's: namely sensor altitude and sensor depression angle. To simplify the model, the sensor depression angle is set at a constant 30 degrees (which is a typical setting for a UAV search profile according to (Souter, 1994)). Search altitude is set at 500 meters to provide a probability of visual and thermal detection of at least 0.9 if the target is in the field of view for the requisite amount of time (Souter, 1994).

a. Search Platform Sensors

The UAV's carried a combination of infrared and optical sensors. Sensors 14 and 15 were type 3 and 4 forward looking infrared receivers with field of views of 10 and 15 degrees respectively. Janus uses type 3 thermal sensors to model early FLIRs in the 3 - 5 μm range, and type 4 thermal sensors to model modern FLIR systems in the 8 - 12μm. Sensors 41 and 43 were type 2 optical TV sensors with fields of view of 10 and 9 degrees. (No type 1 sensors were used since they model the human eye only). The sensor numbers are used in Janus to identify particular systems and are used here to do exactly the same thing.

2. Search Targets

Mobile missile launchers were chosen as the search targets. Mobile missiles are carried on transporter erector launchers (TEL's) which are typically 40 feet long, 12 feet high, and 15 feet wide. A TEL weighs about 29000 kg. So, there should be no problem with the target size adversely affecting target acquisition.

3. Search Methodology

The only desired impediments to target acquisition for our study are weather effects. Thus our search scenario takes place on artificially flat terrain, so that terrain features do not interfere with sensor performance. There are five target TELs, four of which move for a portion of the search, and they are distributed around the perimeter of a 25 km^2 area. Figure 13 shows a layout of the targets and their travel routes.

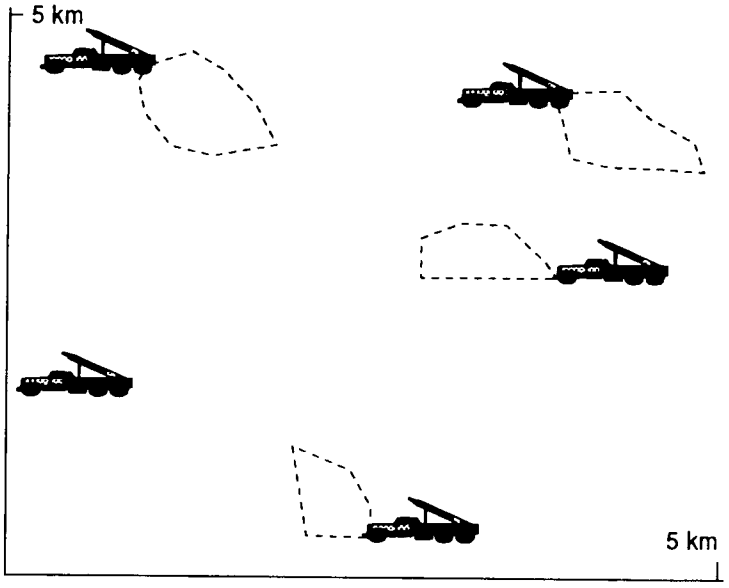

Figure 13: Target TEL Distribution in Search Area

The UAVs perform a random search of the target area, concentrating on the perimeter. Figure 14 shows the target area with the UAV search pattern overlaid.

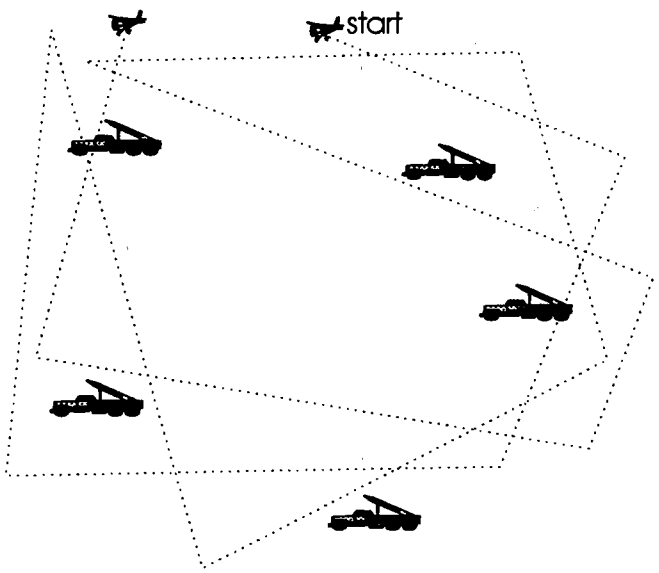

Figure 14: UAV Search Plan

During the simulation, the UAVs were flown in a very close in-line formation at the same altitude. The reason for this formation is that it allows simultaneously acquisition of the same target giving all sensors the same target detection opportunities. The simulation search pattern takes 40 minutes to complete with the UAVs flying at a nominal speed of 65 knots.

4. Scenario Weather

The weather conditions were chosen to examine the effects of the SGR in relatively clear air with little restrictions to visibility, and in a fog-type environment where glare may be

a real factor in acquiring the target. Figure (15) shows the "clear" weather selection that was used.

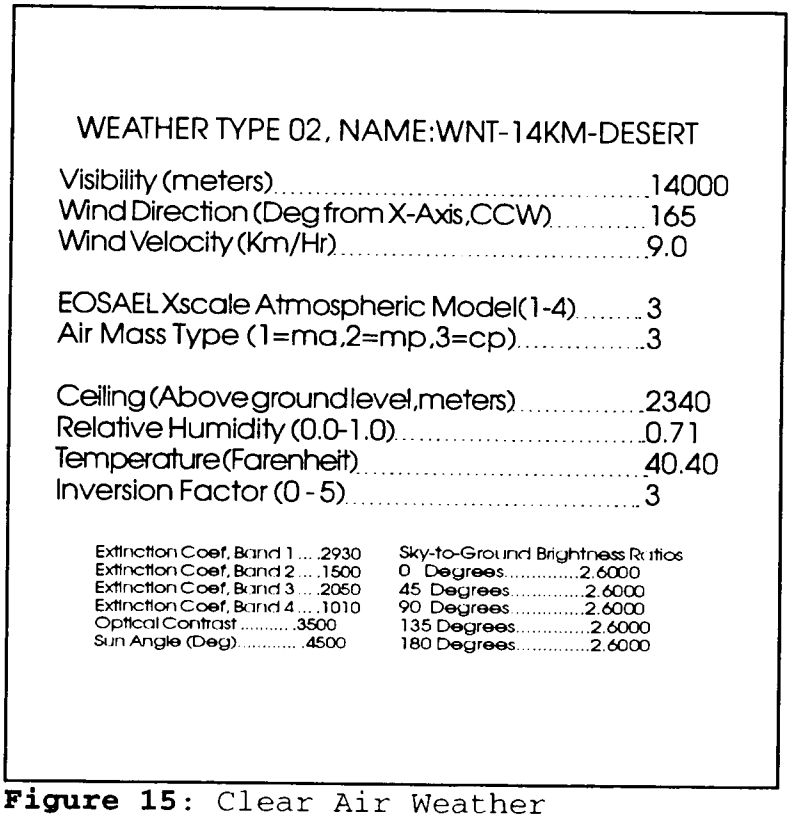

Figure 15: Clear Air Weather

Figure (16) shows the fog weather selection that was used.

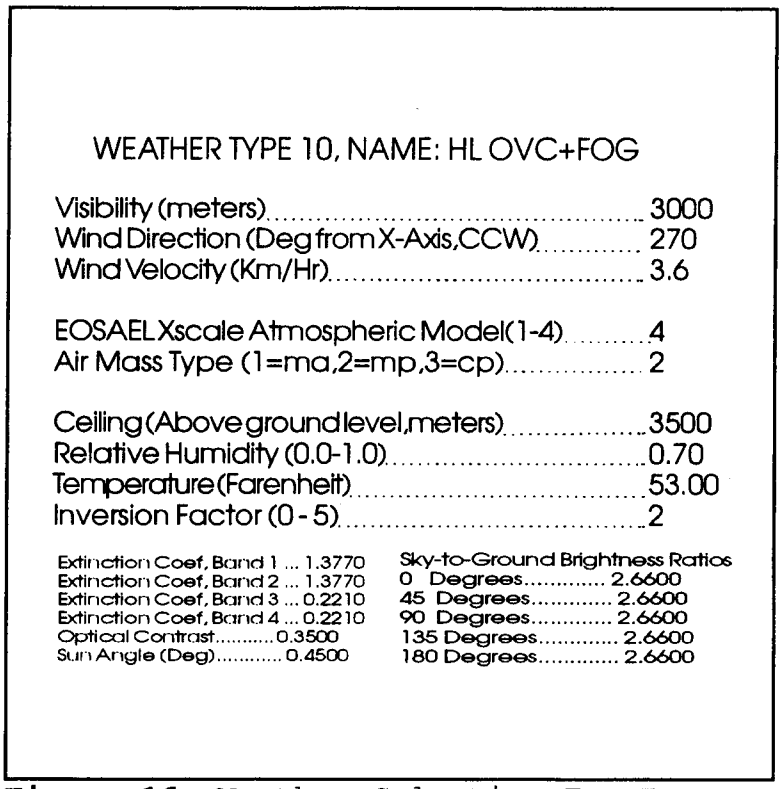

Figure 16: Weather Selection For Fog

The values of all the parameters in the weather selections are those suggested by Janus. Notice that Janus recommends the same SGR factor for both conditions. The value of SGR chosen represents a sun angle of 60 degrees above the horizon. The highest SGR that Janus ever recommends on any of its preset weather conditions is 5.8 (sun angle of 45 degrees). The use of the Janus preset weather conditions would therefore not accurately simulate a dawn attack.

D. SIMULATION RESULTS

Twenty-five simulation runs were performed for each weather condition (five runs at each selected value of SGR).

Figures (17) - (22) show the results of these simulations. They reveal the number of detections versus SGR for clear weather and fog, and the maximum and minimum detection ranges for each optical and thermal sensor versus SGR.

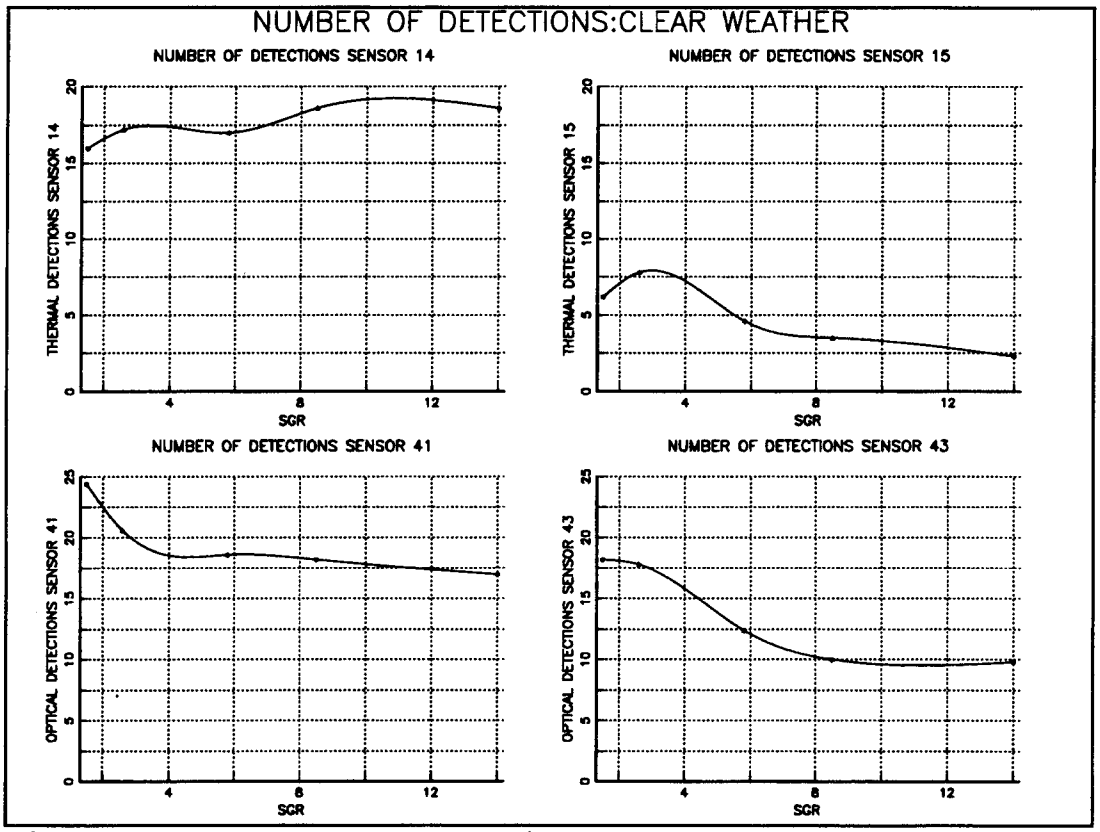

Figure 17: Number of Detections All Sensors Clear Weather

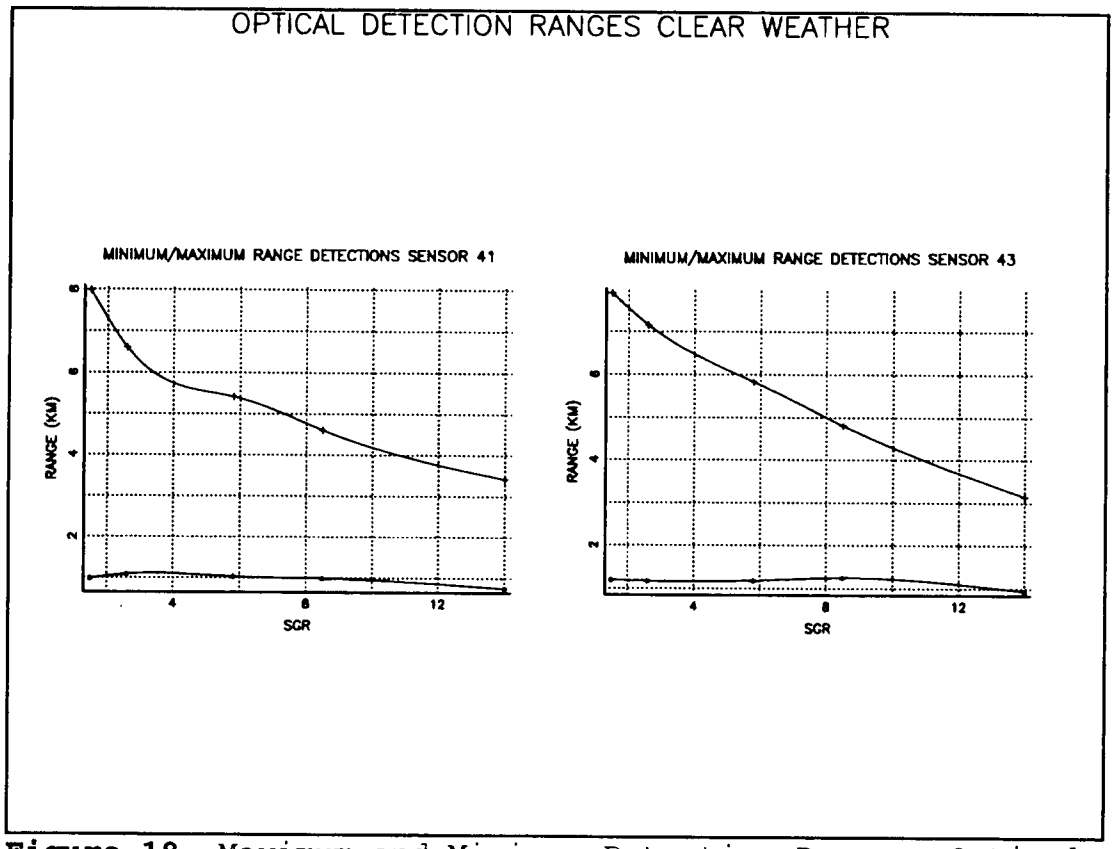

Figure 18: Maximum and Minimum Detection Ranges; Optical, Clear

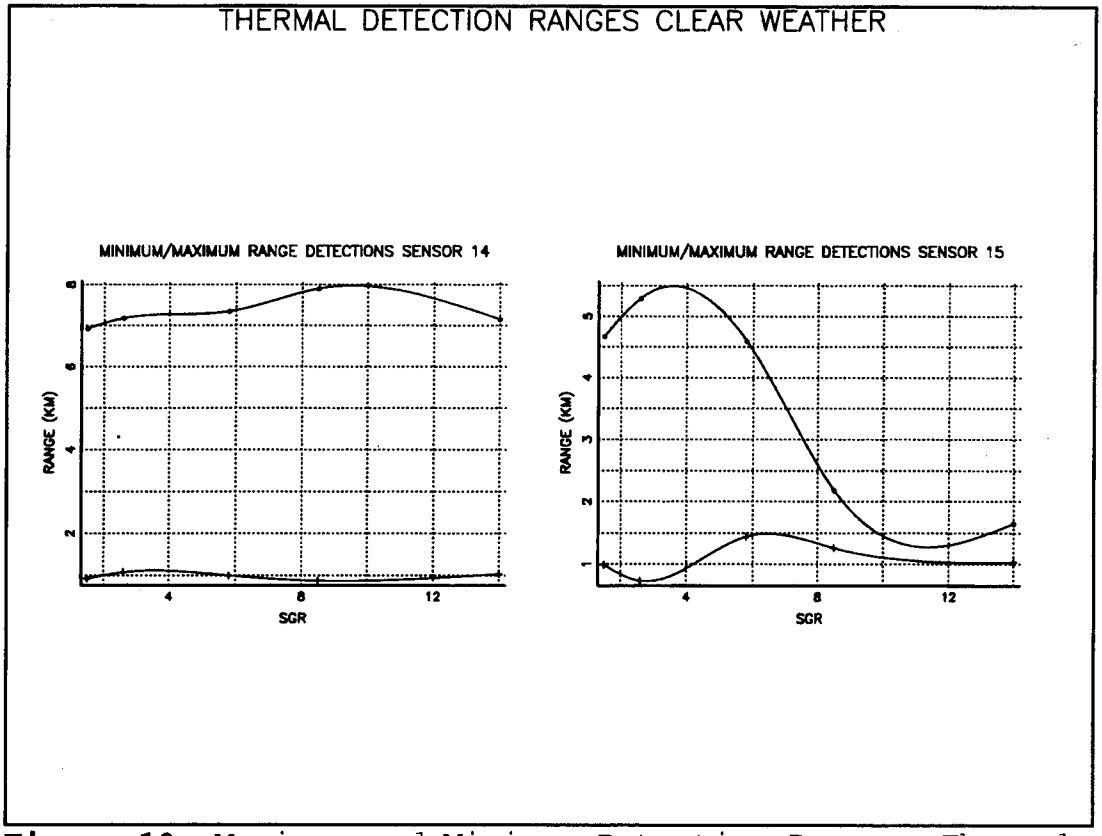

Figure 19: Maximum and Minimum Detection Ranges; Thermal, Clear

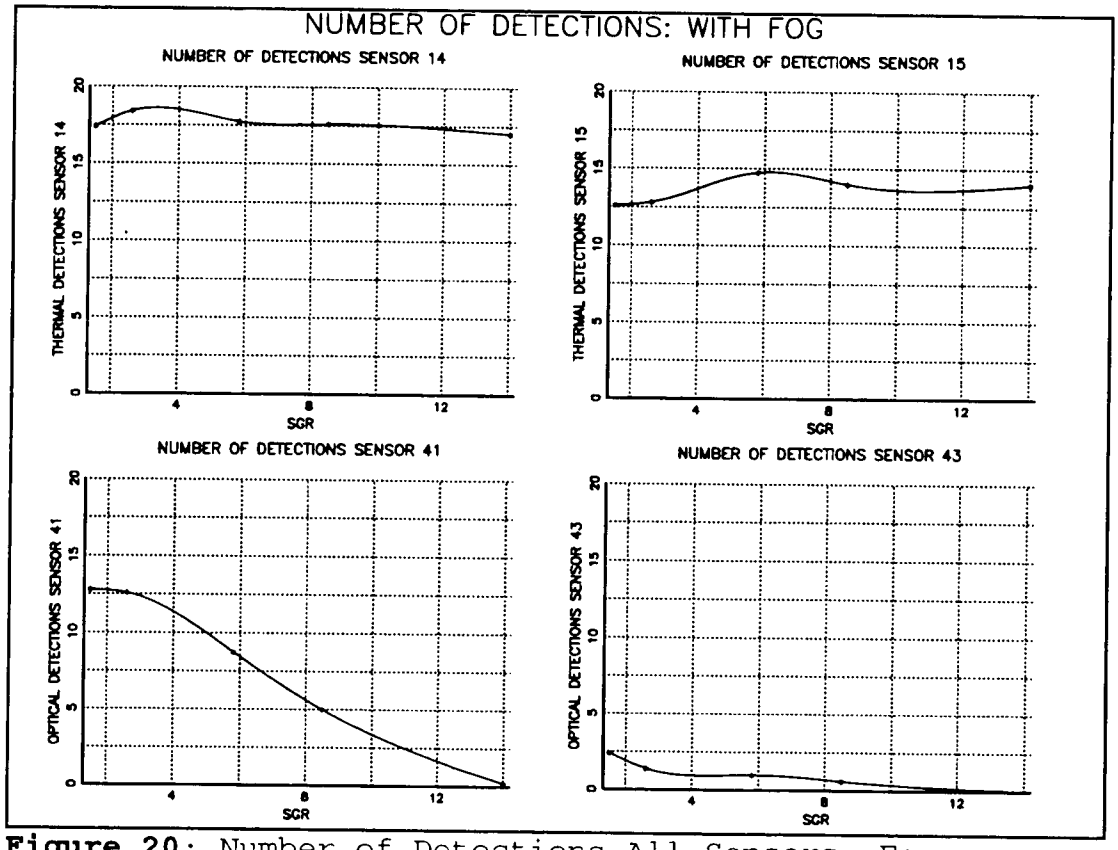

Figure 20: Number of Detections All Sensors: Fog

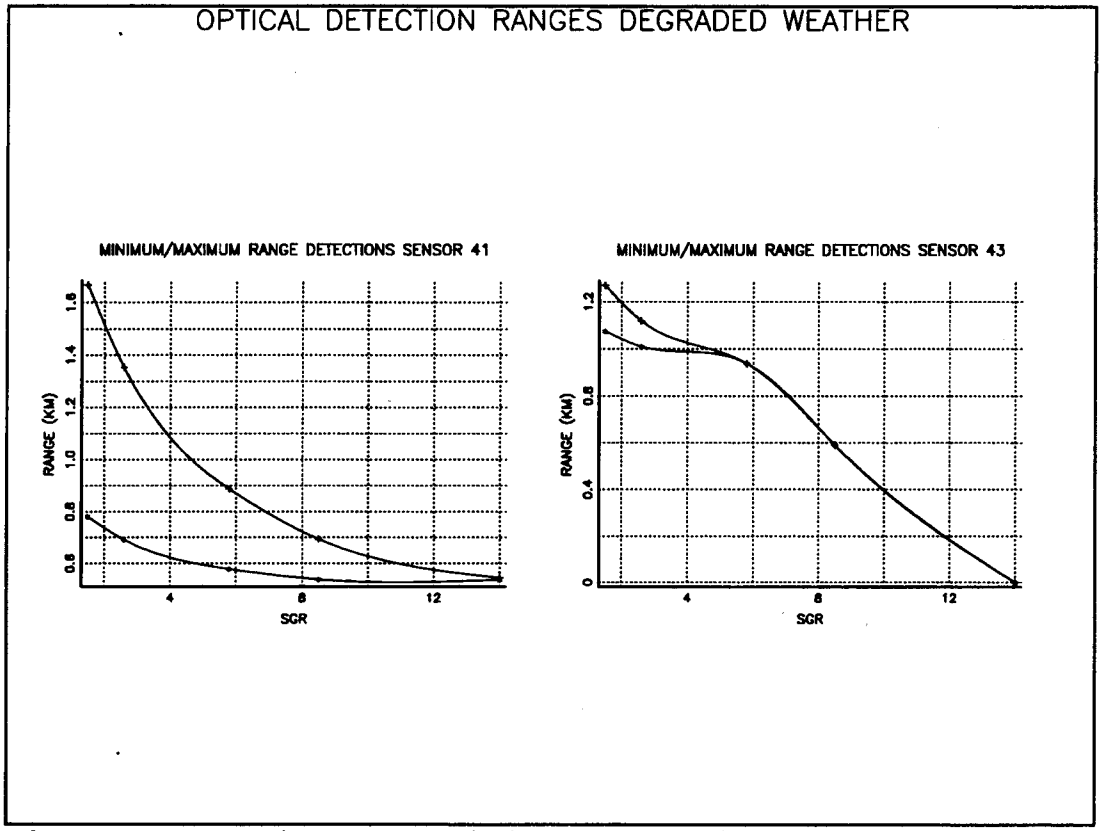

Figure 21: Maximum and Minimum detection Ranges; Optical, Fog

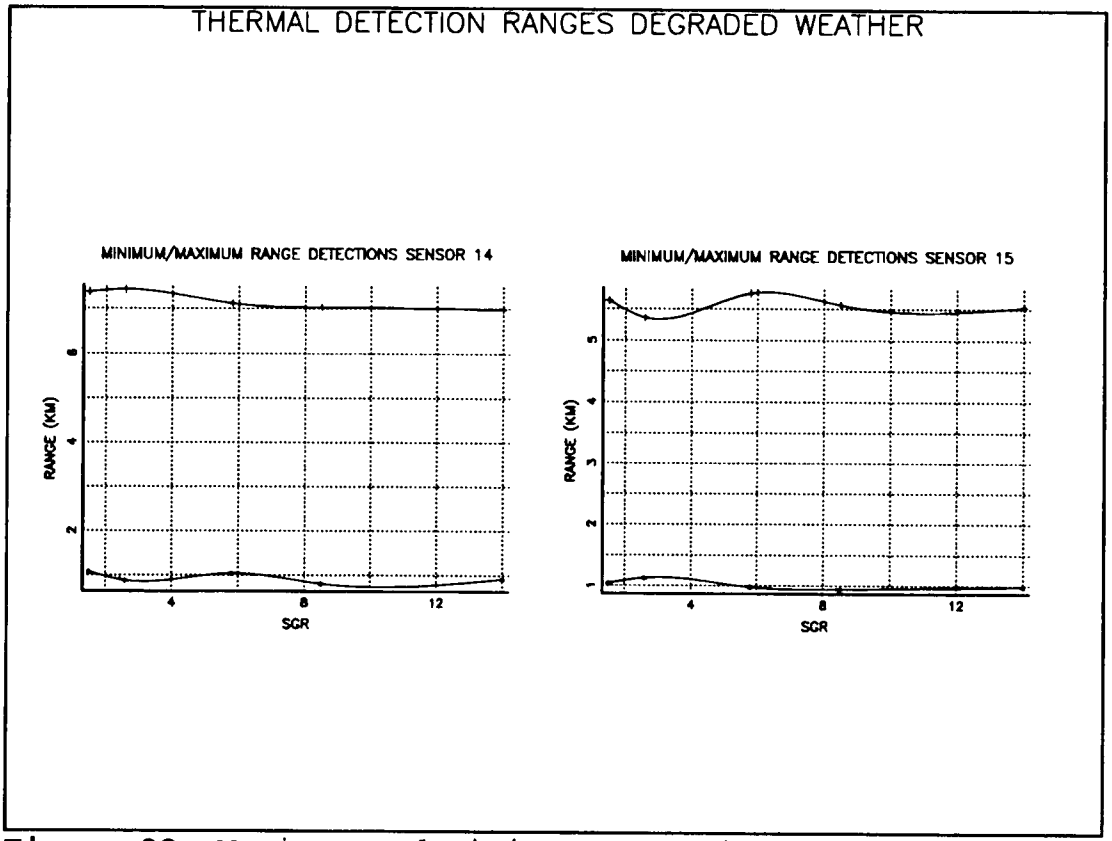

Figure 22: Maximum and Minimum Detection Ranges; Thermal, Fog

As predicted, variation of the SGR significantly affects the number and range of target detections. In clear visibility, increasing SGR from the 2.6 value recommended by Janus has a pronounced impact on the number and range of optical detections. Table III shows the impact of increasing SGR on the number of detections.

Table III: Reduction in Optical Detections: Clear

Percentage Reduction in Optical Detections Clear Weather		
SGR	SENSOR 41 % Reduction	SENSOR 43 % Reduction
1.5	0	0
2.6	15.6	2.2
5.8	23.8	31.9
8.5	25.4	45.1
14.0	30.3	46.2

Referenced to the minimum SGR of 1.5
(Sun angle 90 Degrees)

Table IV displays the impact of increasing SGR on the maximum detection range.

Table IV: Reduction from the Maximum Detection Range

Percentage Reduction Maximum Detection Range: Clear		
SGR	SENSOR 41 % Reduction	SENSOR 43 % Reduction
1.5	0	0
2.6	17.3	9.3
5.8	32.2	25.9
8.5	42.3	39.0
14.0	57.2	60.1

Referenced to the minimum SGR of 1.5
(Sun angle 90 Degrees)

The results for fog are also quite impressive. Even with the minimum SGR, the number of detections was significantly reduced (down from a maximum of 24 to a maximum of 12) due simply to the chosen weather conditions. Under fog conditions, over 14 optical detections is acceptable with SGR at 1.5. Table V shows the detrimental effects on detections due to increasing the glare in a fog environment. Notice that at the highest test value (14.0) optical detections are all but eliminated.

Table V: Reduction Optical Detections:Fog

Percentage Reduction in Optical Detections Fog		
SGR	SENSOR 41 % Reduction	SENSOR 43 % Reduction
1.5	0	0
2.6	1.5	41.7
5.8	31.6	58.3
8.5	60.9	58.3
14.0	92.2	100.0

Referenced to the minimum SGR of 1.5
(Sun angle 90 Degrees)

Table VI is the reduction in maximum detection range caused by increasing SGR.

Table VI: Reduction from the Maximum Detection Range: Fog

Percentage Reduction Maximum Detection Range: Fog		
SGR	SENSOR 41 % Reduction	SENSOR 43 % Reduction
1.5	0	0
2.6	18.8	11.8
5.8	46.8	26.1
8.5	58.4	53.5
14.0	67.4	100.0

Referenced to the minimum SGR of 1.5
(Sun angle 90 Degrees)

IV. CONCLUSIONS

A. WEATHER MODELS

1. XSCALE Model

XSCALE is a tested and validated model. It has the ability to represent well the weather effects required by Janus. The main use of XSCALE by Janus is to determine target acquisition extinction coefficients for inclined lines of sight. As discussed in Chapter II, XSCALE can represent virtually any weather condition that is required by Janus for its slant range calculations.

2. Inversion Factor Model

The inversion factor model is based on the PSC method for estimating atmospheric stability. The model controls the rate of growth of smoke and dust clouds, but itself has little to do with the optical target detections.

3. Sky-to-Ground Brightness Ratio Model

SGR, as modeled in Janus, influences both the number and the range of optical detections under clear and degraded weather conditions. Therefore SGR has a significant impact on optically guided weapons or optical detection systems. The current SGR model is valid only on the zero relative bearing (from the observer's nose).

B. RESULTS OF SEARCH SCENARIO

The search scenario verified the SGR effect on optical sensors. In clear weather there was shown to be a significant decrease in target detections and acquisitions as SGR was increased to its highest value. Under fog conditions, where glare becomes a real factor for optical sensors, the results were quite dramatic. Only one optical detection was made at the highest value of SGR, and detection ranges were reduced to just over 500 meters in fog (with 3000 meters prevailing visibility). Janus does not currently model the sun's angle of inclination. However, a "sun in the eyes" effect can be simulated to some degree by using SGR.

As predicted changing the SGR has little effect on thermal sensors. The number of thermal detections and their detection ranges were basically unaffected by increasing SGR, with the sole exception of sensor 15 in clear weather. These thermal detection results also demonstrate that varying SGR does not cause the simulation to crash.

1. Recommendations

There are current plans to implement SGR on the 0,45, 90, 135 and 180 degree relative bearings. This implementation should increase the fidelity of the simulation in low sun angle combat simulations, (which is important since many tactics employ early morning or dusk assaults).

To take advantage of the SGR effect, it is recommended that Janus implement sun angle in order to realistically play a "sun in the eyes" versus a "sun at back" type scenario. There are occasions where that tactic is desirable based on the enemy's technical limitations, (such as when it depends on optical technology or has only limited thermal imaging capabilities).

C. PROPOSED FURTHER STUDY

The next logical step would seem to be employment of SGR in a combat scenario where detection and target attack are the goals. The weapons used should be a mix of optically guided and thermally-guided weapon systems. It would also be very useful to collect data from actual exercises in order to update and improve the simulation model.

LIST OF REFERENCES

Bohren, Craig F., and Huffman, Donald R., *Absorption and Scattering of Light by Small Particles*, John Wiley & Sons, New York, 1983.

Deirmendjian, D., Scattering and Polarization Properties of Water Clouds and Hazes in the Visible and Infrared, *Applied Optics*, vol. 3, pp. 187 - 196, 1964.

Fiegel, R.P., *Natural Aerosol Extinction Module XSCALE 92 User's Guide*, U.S. Army Research Laboratory, Battlefield Environment Directorate, White Sands Missile Range, NM 88002-5501, 1994.

Hanel, G., The Properties of Atmospheric Aerosol Particles as Functions of the Relative Humidity of Thermodynamic Equilibrium with Surrounding Moist Air, *Advances in Geophysics*, vol. 19, Academic Press, New York, pp. 73 - 188, 1976.

Heaps, Melvin G., *A Vertical Structure Algorithm for Low Visibility/Low Stratus Conditions*, ASL-TR-0111, U.S. Army Atmospheric Sciences Laboratory, White Sands Missile Range, NM 88002, 1982.

Heaps, Melvin G., and Johnson R.D., *An Algorithm for the Vertical Structure of Aerosol Extinction in the Lowest Kilometer of the Atmosphere*, ASL-TR-0142, U.S. Army Atmospheric Sciences Laboratory, White Sands Missile Range, New Mexico 88002-5501, 1983.

Hoock, Donald, *Weather, Propagation, and Target Acquisition* Lecture Slides, U.S. Army Research Laboratory, Battlefield Environment Directorate, White Sands Missile Range, New Mexico, 1994.

Janus Users' Manual, W800XR-3125-0052:5/05/93, Department of Army Headquarters TRADOC Analysis Center ATRC-ZD, Fort Leavenworth, Kansas 66027.

Joint Technical Coordinating Group for Munitions Effectiveness (JTCG/ME), *Standards for Large-Area Screening Systems (LASS) Modeling*, 61 JTCG/ME-88-6, U.S. Army Material Systems Analysis Activity, Aberdeen Proving Ground, MD 21005-5701, 1990.

Lindberg, James D.,*Early Wintertime Fog and Haze Report on Project Meppen 80*,ASL-TR-0108, U.S. Army Atmospheric Sciences Laboratory, White Sands Missile Range, NM 88002, 1982.

Lindberg, James D.,*Final Report on the European Vertical Structure Experiment at Cardington, England*,ASL-TR-0153, U.S. Army Atmospheric Sciences Laboratory, White Sands Missile Range, NM 88002, 1984.

Lindberg, James D.,and Loveland, Radon B.,and Duncan Louis D., and Richardson M.B.,*Vertical Profiles of Extinction and Particle Size Distribution Measurements Made in European Wintertime Fog and Haze*,ASL-TR-0151, U.S. Army Atmospheric Sciences Laboratory, White Sands Missile Range, NM 88002, 1984.

Seagraves, Mary Ann,*Visible and Infrared Extinction due to Falling Snow: An Approximate Model*,ASL-TR-0158,U.S. Army Atmospheric Sciences Laboratory, White Sands Missile Range, NM 88002,1984.

Shettle, Eric P., and Fenn R.W.,*Models for the Aerosols of the Lower Atmosphere and the Effects of Humidity Variations on Their Optical Properties*, AFGL-TR-79-0214, Air Force Geophysics Laboratory, Hanscom Air Force Base, MA 01731, 1979.

Souter, Paul, *On the Use of Unmanned Aerial Vehicles to Search for Tactical Ballistic Missile Transporter-Erector-Launchers*, Master's Thesis, Naval Postgraduate School, Monterey, CA 93943-5000, 1994.

Waldvogel, A.,The N_0 Jump of Raindrop Spectra,*Journal of Atmospheric Science*,vol. 31, pp.1067 - 1078, 1974.

INITIAL DISTRIBUTION LIST

		No. Copies
1.	Defense Technical Information Center Cameron Station Alexandria VA 22304-6145	2
2.	Library, Code 052 Naval Postgraduate School Monterey CA 93943-5002	2
3.	Professor Bard Mansager, Code MA/Ma Department of Mathematics Naval Postgraduate School Monterey, CA 93943	1
4.	Professor Maurice Weir, Code MA/Wc Department of Mathematics Naval Postgraduate School Monterey, CA 93943	1
5.	CPT Charles Pate, USA TRAC-Mtry Naval Postgraduate School Monterey, CA 93943	1
6.	Chairman Department of Mathematics Naval Postgraduate School Monterey, CA 93943	1
7.	Vincient F. Shorts 107 Heather Court Vallejo, CA 94591	1